 doi:10.20944/preprints202207.0278.v1

Article

Biodiesel Synthesis from Milk Thistle Extract of *Silybum marianum* (L.) Gaertn. using ZnO Nanoparticles as A Catalyst

Hammad Ahmad Jan[1], Igor Surina[2]*, Ahmed Al-Fatesh[3], Abdulaziz M. Almutlaq[3] and Sher Wali[4]

[1] Department of Botany, University of Buner, Buner, Pakistan, (hammadjan@ubuner.edu.pk)
[2] Department of Wood, Pulp and Paper, Institute of Natural and Synthetic Polymers, Faculty of Chemical and Food Technology, Slovak University of Technology in Bratislava, Radlinského 9, 812 37 Bratislava, Slovakia, (igor.surina@stuba.sk)
[3] Chemical Engineering Department, College of Engineering, King Saud University, P.O. Box 800, Riyadh 11421, Saudi Arabia, (aalfatesh@ksu.edu.sa) (mutlaq@ksa.edu.sa)
[4] Department of Botany, Islamia College Peshawar, Pakistan, (sherwali@icp.edu.pk)
* Correspondence: Igor Šurina, e-mail: igor.surina@stuba.sk

Abstract: Biodiesel is considered valuable to reduce dependency on petro-fuels. This work aimed to synthesize biodiesel from *Silybum marianum* using synthesized ZnO nanoparticles as a catalyst. The synthesized ZnO nanoparticles were examined by scanning electron microscopy and X-ray diffraction for confirmation. The synthesized biodiesel was confirmed by ASTM D-6751, H and C-NMR, GC-MS, and FT-IR spectroscopy. The optimal biodiesel yield of 91% was obtained in the oil-to-methanol ratio of 1:24, 15 mg of catalyst concentration, 60 ^{0}C temperature, and 45 minutes of reaction time. Fuel properties were determined according to the ASTM defined methods and found within the defined limits of ASTM D-6751. *^{1}H-NMR* and *^{13}C-NMR* showed characteristic peaks at 3.667 ppm, 2.000 to 2.060 ppm, 0.858-0.918 ppm, 5.288-5.407 ppm, 24.93-34.22 ppm, 172.71, 173.12, 130.16 ppm, and 128.14 ppm, respectively, which confirm biodiesel synthesis. The FAMEs composition of biodiesel was determined by GC-MS which recognized 19 peaks for different types of FAMEs. FT-IR spectroscopy showed two main peaks, first in the range of 1725-1750 cm^{-1} and second in the range of 1000-1300 cm^{-1}, which confirmed that the transesterification process was completed successfully. The physicochemical characteristics of *Silybum marianum* confirm that it is a suitable source to produce biodiesel on industrial scale.

Keywords: biodiesel synthesis; nanoparticle synthesis; green catalyst synthesis; physicochemical analysis; *Silybum marianum*; nonedible feedstock

1. Introduction

Currently, the world is confronting an intense shortage of petrofuels. In this scenario, the demand for alternative energy resources is increasing and is time-consuming. Biodiesel is considered valuable because of the reduction in demand for petrofuels and is economically important. Furthermore, biodiesel is environmentally friendly because it reduces greenhouse gas emissions, and it is also important socially, due to the generation of new employment and income opportunities [1]. It can be synthesized from animal fats or vegetable oils using the transesterification technique. In this technique, alcohol and fats or oil are reacted in the presence of catalyst at a specific temperature, resulting in the formation of fatty acid methyl esters (FAME) [2,3]. However, the use of oil obtained from plants is a competitor source for biodiesel production compared to animal fats [4].

In the presence of either a base or an acid catalyst, the biodiesel synthesis process is carried out efficiently. There are two main disadvantages, i.e., equipment corrosion and slower reaction rate, which makes acid catalysts not suitable for commercial purpose. However, base catalysts are much more efficient due to the higher rate of reaction (4000 times more) compared to acidic catalysts [5]. Although base catalysts are widely available and cheap, base catalysts still have one main drawback, these catalysts work best when

Preprints (www.preprints.org) | NOT PEER-REVIEWED | Posted: 19 July 2022 doi:10.20944/preprints202207.0278.v1

the oil has a free fatty acid (FFA) content below 0.5%, at higher concentrations of FFA their catalytic activity is reduced [6]. However, biodiesel synthesis is commonly carried out on an industrial scale in the presence of homogeneous catalysts (sodium hydroxides or alkoxides). But homogeneous catalysts have some limitations; for example, homogeneous catalysts are not recyclable and are not environmentally friendly by forming biodiesel polluted with potassium or sodium ions [7]. Furthermore, these catalysts also favor more soap formation during biodiesel synthesis. Moreover, homogenous catalysts become less active when the feedstock has more humidity than 0.3 wt.% [8]. Thus, these catalysts need pure raw materials from feedstocks to synthesize biodiesel.

The feedstock such as animal fats, cooking oils, non-disable plant oils etc. were used as a feedstock to synthesize biodiesel because these feedstocks are less expensive [9]. But the main problems with these feedstocks are their high humidity (~3% by weight) and FFA content (up to 12%) which for the synthesis of biodiesel does not favor the use of homogeneous catalysts. To solve this problem, researchers have synthesized nanocatalysts which have many advantages over homogeneous catalysts, such as their good performance as a catalyst and recyclability at the end of reaction. Furthermore, these catalysts maintain their activity even at high FFA content and humidity of the feedstock [7]. Furthermore, compared to ordinary catalysts, nanocatalysts are more effective because of their ultra-small size (10–80 nm) that provides a substantial surface area to volume ratio, and nano-sized materials have characteristics that they do not have when the same materials are in macroscopic size [10]. Furthermore, the catalytic activity of a nanoparticle is significantly influenced by its size and distance between the nanoparticles [7].

Silybum marianum (L.) Gaertn., commonly known as milk thistle, is an annual herb of the family Asteraceae. The plant is native to the Mediterranean region of Europe but is commonly found in the subtropical and temperate region of Pakistan. The plant grows in the wild and also as a weed in a wheat crop field. The plant grows to a height of 1-2m. The stem of the plant is glabrous. The leaves are oblong to lanceolate, shiny green, have milky white veins, and spines on the edges. The flower heads are 4-12cm long and wide and have a red or purple color. The flower heads are surrounded by bracts, which are hairless and with triangular spiny edges. The seeds of the plant start germination in October and continue through December. The plant produces seeds from February to March [11]. This study aimed to synthesize biodiesel from milk thistle (*Silybum marianum* (L.) Gaertn.) using green synthesized ZnO nanoparticles as catalyst.

2. Materials and Methods

2.1. Extract Preparation

Fresh plant materials from *Silybum marianum* were taken and washed three times with double distilled water to eradicate dust and pollution. The cleaned materials were kept in an oven at 60 ^{0}C for 30 minutes to dry. The dried leaves were ground to fine powder in a Panasonic miller grinder. The 15 g of powdered plant material was then boiled (100 ^{0}C) in 120 ml of deionized water for one hour with constant stirring on a hot plate. The color of the extract obtained was dark green. The mixture was then cooled to room temperature. This solution was filtered three times through Whatman filter paper-42. The pH of the extract was 5.9. The extract was stored in the refrigerator at 4 ^{0}C for future use [12,13].

2.2. ZnO Catalyst Synthesis

Hydrated zinc nitrate Zn $(NO_3)_2.6H_2O$ of analytical grade (Merck) was used as a zinc precursor. Approximately 100 ml of the plant material extract was taken in the conical flask and 6 g of zinc nitrate was added to it. The mixture was boiled (100 ^{0}C) under constant stirring on hotplate for until a light-yellow color suspension was formed. The precipitate was washed three times with deionized water and centrifuged at 1000 rps for 10 minutes. Subsequently, it was calcined in the furnace at 450 ^{0}C for two hours. A pale white

Preprints (www.preprints.org) | NOT PEER-REVIEWED | Posted: 19 July 2022 doi:10.20944/preprints202207.0278.v1

crystalline powder of ZnO was obtained after calcination. The powder was stored carefully for further analysis [12,13].

2.3. Catalyst Characterizations by XRD and SEM

XRD (Model No. D8 Advance Bruker) was used for the characterization of catalysts used in the present work to safeguard the establishment of a desired crystal-like assembly of all nanoparticles. With the help of the Scherer equation, the calculation was completed, providing a heterogeneous ordinary diameter of the nanoparticles. All dimensions were achieved between (10 - 60°C). XRD analysis was performed at 2θ with a range of (10°-90°) using a SHIMADZU 6000 diffractometer equipped with a Cukα (K=1.54 A°) source, maintaining an applied voltage of 40 kV and a current of 30 mA. SEM was achieved using SEM, Model JEOL JSM-5910, & HT7800 Ruli. Scanned images were obtained by operating-field emissions from a SEM microscope with (20 kV) accelerating voltage. It aided in the interpretation of the phenomena that occurred during calcination and pretreatment and permits qualitative characterization of the surface of catalysts.

The magnitude of the XRD points of the sample reveals that the designed nanoparticles remain crystalline and wide-ranging diffraction peaks specify the very small crystallite [21].

$$D = \frac{k\lambda}{\beta \cos\theta} \quad (1)$$

where k is the shape factor = 0.9, λ is the radiation wavelength (1.54 Å), β is the full width of half of the maximum intensity (FWHM) in radians.

2.4. Oil Extraction from Feedstock

The seeds were collected from various parts of the Tehsil Khadukhel district in Buner, northern Pakistan. The collected seeds were washed with half-warm distilled water to remove the dust and then dried in the oven at 50 °C. 10 g of dried seeds were finely powdered in pastel mortar. This fine powder was then subjected to the Soxhlet apparatus for the chemical extraction of oil using ether as the solvent. After extraction, the solvent was recycled with the help of a rotary evaporator at 55 °C under moderate vacuum. The total oil content of the feedstock was then calculated with the help of the mathematical formula given below [14];

$$Oil\ contents\ percentage\ W4 = \frac{W3+W1}{W2} \quad (2)$$

whereas

W_1 is used for the weight of empty flask, W_2 for the weight of the seed powder before extraction, W_3 is used for the weight of the flask and oil extracted, and W_4 is the weight of oil extracted through soxhlet from the seed powder of feedstock.

The chemical extraction was followed by the mechanical extraction of oil from the feedstock to extract oil in a bulk amount. The oil was extracted using an electrical expeller Model YZS-130A/C. The crude oil was filtered three times using Whatman filter paper N.42 and stored in a glass jar for further experimental work [15].

2.5. Free Fatty Acids Content Determination

The crude oil was analyzed for FFA contents to make an appropriate adaptation of the method for the synthesizing of biodiesel. The FFA content was determined using the Ullah et al. titration method [15]. After titration, the FFA content of the feedstock was calculated to be 0.74 mg KOH/g with the help of the formula given below;

$$Percentage\ of\ FFA = \frac{(A-B)\times C}{V} \times 100 \quad (3)$$

whereas

A = potassium hydroxide (KOH) volume used in the sample titration.

Preprints (www.preprints.org) | NOT PEER-REVIEWED | Posted: 19 July 2022 doi:10.20944/preprints202207.0278.v1

B = potassium hydroxide (KOH) volume used in blank titration.
C = potassium hydroxide (KOH) concentration (g/l).
V = volume of oil sample.

2.6. Biodiesel Synthesis Process

To synthesize biodiesel, we have adopted the transesterification method, as the FFA content of feedstock is 0.74 mg KOH/g. The biodiesel yield in percent after the end of the experiment was calculated by using the following formula [16];

$$Percentage\ yield\ of\ Biodiesel = \frac{Biodiesel\ produced}{Oil\ sample\ used\ in\ reaction} \times 100 \quad (4)$$

2.7. Fuel Properties Determination

Following fuel properties were determined for biodiesel synthesized from *Silybum marianum*: acid value (KOH mg/kg), Flash Point ^{o}C (PMDC), density at 15 ^{o}C (kg/l), kinematic viscosity at 40 ^{o}C CST, Pour Point ^{o}C, Cloud Point ^{o}C, Sulphur % wt, calorific value kJ/kg, Cetane no., oxidative stability 110 ^{0}C (h), Refractive index @ 20 ^{0}C, Iodine number mg I_2/100, higher heating value MJ/kg, and distillation temperature 90% recovery defined by ASTM for biodiesel were analyzed according to the ASTM methods (**Table 1**) [17,18].

Table 1. Fuel properties of the *Silybum marianum* biodiesel and ASTM standard methods values.

Fuel Property	ASTM Methods	[1] ASTM D6751	[2] SMB
Acid value (KOH mg/kg)	ASTM D-664	0.80	0.74
Flash Point PMCC (^{o}C)	D-93	>93	87
Density at 15^{o}C (kg/L)	D-4052	0.820-0.900	0.857
Kinematic Viscosity at 40^{o}C (mm^2/s)	D-445	1.9 - 6	4.69
Pour Point (^{o}C)	D-97-12	-15 to 16	-8
Cloud Point (^{o}C)	D-2500-11	-3 to 12	-2
Sulphur (% wt)	D-5453	0.007	0.00018
Calorific Value (kJ/kg)	D-5865	35000	26984
Cetane no.	D-613	45	49
Oxidative stability 110 ^{0}C (min)	EN-14112	3	2.8
Water content (mg/kg)	ASTM D-6304	≤0.05	0.039
Refractive index (@ 20^{0}C)	ASTM D-1747	----	1.437
Iodine number (mg I_2/100)	ASTM D-4607	≤120	124
Higher heating value (MJ/kg)	ASTM D-240	39-43	40.86
Distillation temperature 90% recovery	ASTM D-1160-06	360	345

1 ASTM D6751 - Value Test Limit, 2 SMB - *Silybum marianum* biodiesel

Preprints (www.preprints.org) | NOT PEER-REVIEWED | Posted: 19 July 2022 doi:10.20944/preprints202207.0278.v1

2.8. Chemical Assessment of Biodiesel Synthesis

FT-IR, GC-MS, and NMR spectroscopic analyses were performed to confirm the synthesis and to study of the chemical properties of SMB.

2.9. Fourier Transform Infrared Analysis of SMB

FT-IR spectroscopy was performed using the VARIAN AA280Z atomic absorption spectrometer with GTA-120 graphite tube atomizer in the range of 400-4000 cm^{-1} for confirmation of the successful occurrence of the transesterification process and biodiesel synthesis.

2.10. NMR Spectroscopy of SMB

^{1}H and ^{13}C NMR spectroscopic analysis was performed at 21 ^{0}C on 11.75 T using the Avance NEO Bunker 600 MHz spectrometer equipped with a 5 mm BBFO smart probe using chloroform-D and $Si(CH_3)_4$ solvents as internal standard for authentication. To record the ^{1}H NMR (300 MHz) spectrum, the pulse duration was set at 30 °C with the recycle delay of 1.0 scans and 8 scans. Similarly, the ^{13}C NMR spectrum (75 MHz) was recorded with a pulse duration of 30^{0} with a recycle delay of 1.89 and 160 scans. All chemical transformations were reported in ppm relative to the residual solvent peak. The following formula was used to calculate the conversion percentage [19]:

$$Percentage\ of\ Biofuel,\ C = 100\ x\ 2AMe/\ 3ACH_2 \quad (5)$$

whereas,
C = Oil to biodiesel conversion percentage
AMe = methoxy protons' integration value in biodiesel
ACH_2 = α-methylene protons' integration value in biodiesel

2.11. GC-MS determination of FAMEs

The synthesized biodiesel was analyzed both qualitatively and quantitatively for various FAMEs by GC-MS spectroscopy; for this purpose, a model QP 2010 Plus; Shimadzu Japan made spectrometer was used. To analyze the biodiesel, 1 **µl** of sample was injected into GC-MS. Hexane was used as a solvent, and helium was used as a carrier gas. The gas chromatographic separation was carried out at column temperature of 50-300 ^{0}C. Injector and detector temperature were maintained at 250°C.

3. Results and Discussion

3.1. X-ray diffraction of ZnO nanocatalysts

The XRD analysis spectrum obtained for ZnO nanoparticles (**Figure 1**), indicates strong deflection heights at 2-theta angles 31.77, 34.35, 35.86, 47.25 56.50 62.53 66.18, 67.69, 68.76, 72.42 and 76.50 corresponding to (100), (002), (101), (102), (110), (103), (200), (112), (201), (004) and (202) planes, respectively.

Preprints (www.preprints.org) | NOT PEER-REVIEWED | Posted: 19 July 2022 doi:10.20944/preprints202207.0278.v1

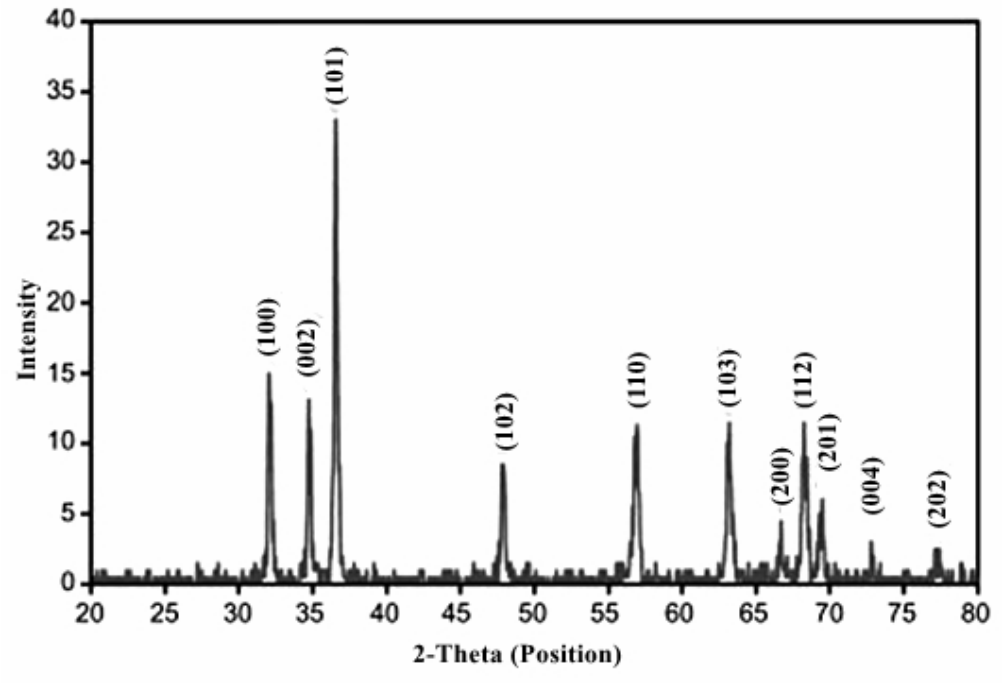

Figure 1. XRD analysis spectrum patterns confirming the ZnO nanoparticles synthesis.

In the XRD pattern, no additional peaks were observed for any other compound of zinc or metallic zinc. Furthermore, the sharpness and intense diffraction of obtained peaks are indications of crystallization of the nanoparticles. These characteristics show that the synthesized substance is pure ZnO nanoparticles [20].

3.2. Scanning Electron Microscopic Study of ZnO

The surface and morphological characterizations of the ZnO nanoparticles were studied by SEM; Jeol Model appliance (JSM-6390LV). The synthesized nanoparticles are spherical in shape and densely packed with a size of 43 nm (**Figure 2**).

Furthermore, the particles have less agglomeration, good connectivity, and homogeneity among the particles. Moreover, the surface of the particles is porous, which may be due to the release of hot gases from the reaction mixture during the combustion process [20,22]. ZnO-ZnO nanoparticles bond to each other due to the presence of nodule formation [23]. The ordered and regular shape of particles is the sign of a better interconnected regular pore distribution system [24].

Preprints (www.preprints.org) | NOT PEER-REVIEWED | Posted: 19 July 2022 doi:10.20944/preprints202207.0278.v1

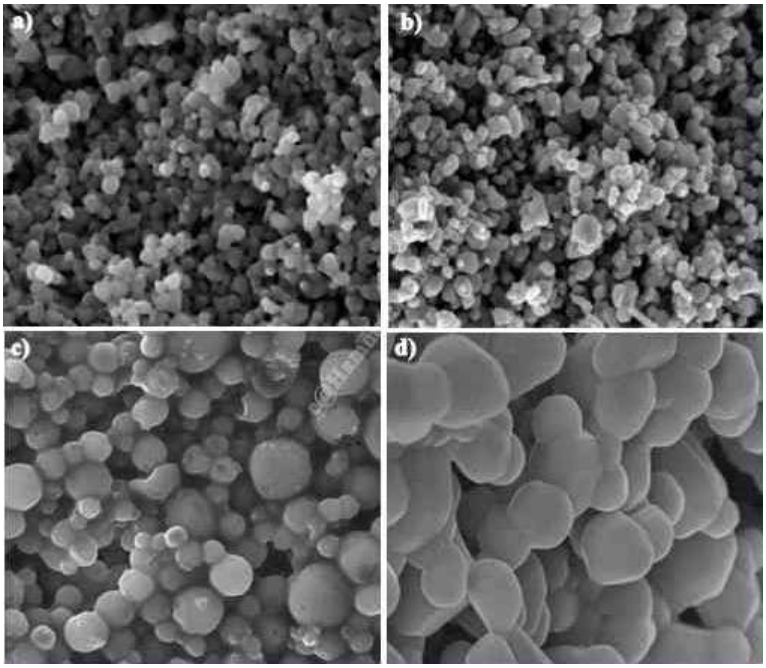

Figure 2. SEM analysis of ZnO nanoparticles confirmimg the synthesis of nanoparticles and size a) 1µm X5,000; b) 1µm X10,000; c) 1µm X20,000; d) 1µm X30,000.

3.3. Oil Extraction and FFAs Content Determination

We have used two approaches (chemical through soxhlet and mechanical) of oil extraction to compare our result with the international standard techniques stated by various researchers in their work. The soxhlet extraction technique is specified by the European Union for the extraction of oil from the feedstock. Furthermore, the use of these techniques is cost-effective and easy to handle [15]. The oil content in the feedstock used in this work was 45.2%. Other researchers have also reported almost same results [17,25]. Furthermore, the FFA contents were also determined through the acid titration method prior to the biodiesel synthesis process. The FFA content is reported as 0.74mg of KOH/g, which is below the internationally specified limit. If the feedstock content of FFA exceeded 3%, the oil to biodiesel conversion efficacy declined gradually [15].

3.4. Biodiesel Synthesis and Optimization

To determine conditions suitable for maximum biodiesel yield, a series of experiments were accomplished considering four main reactions variables, i.e., the oil-to-methanol ratio, catalyst concentration, reaction time, and temperature.

3.4.1. Oil-to-methanol ratio

The oil to methanol ratio has a profound effect on the biodiesel yield, increase in the amount of methanol with respect to oil increases the biodiesel yield [25,15]. Therefore, we have also varied the oil to methanol ratio, that is, 1:6, 1:12, 1:18, 1:24, and 1:30. The reported results clearly showed that the highest biodiesel yield was obtained at 1:24 oil/methanol ratio. (**Figure 3**). Other researchers reported almost similar results [15,25,26]. Furthermore, according to the literature, the minimum stoichiometric molar ratio for transesterification of alcohol to oil is 3:1.

Preprints (www.preprints.org) | NOT PEER-REVIEWED | Posted: 19 July 2022 doi:10.20944/preprints202207.0278.v1

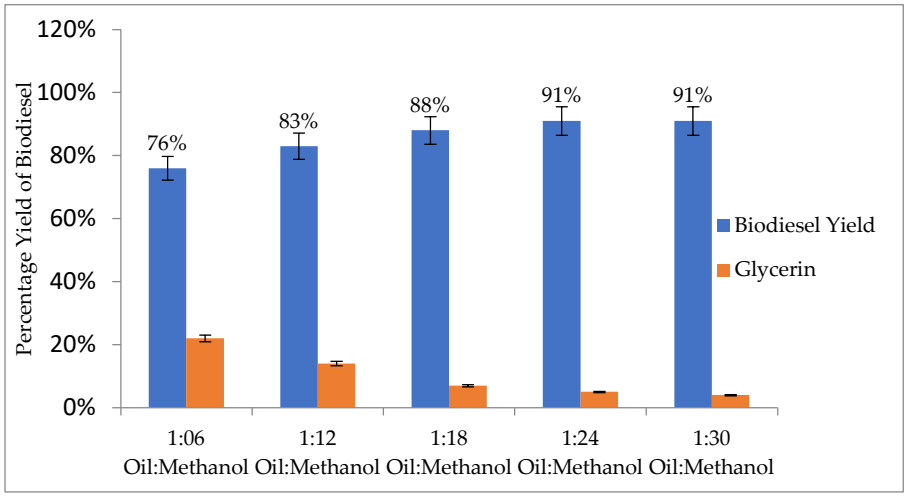

Figure 3. Oil to methanol ratio has positive effect on biodiesel yield and negative on glycerin formation.

However, as the transesterification reaction is reversible, therefore, a higher molar ratio enhances the miscibility as well as the interaction among the triglycerides and alcohol molecules. According to the literature, for the completion of the reaction or maximum biodiesel yield, the molar ratio would be kept higher than the stoichiometric ratio [27]. To break the links among glycerin and fatty acids during the transesterification reaction, the presence of an adequate amount of methanol is desirable [28]. However, a very high amount of methanol must be avoided because higher oil-to-methanol ratios cannot optimize the biodiesel yield and esters contents; however, it complicates the ester recovery process and increases the cost [15]. Furthermore, in the biodiesel synthesis process, a high amount of methanol of more than 1:70 molar ratio slows the separation of glycerol and ester [29].

3.4.2. Catalyst Concentration

The catalyst plays an important role in biodiesel yield; the efficient conversion of oil to methyl ester during transesterification is only possible in the presence of a suitable catalyst [25,30]. In this work, we studied the influence of catalyst concentration by keeping concentration 5 mg, 10 mg, 15 mg, 20 mg, and 25 mg to get the optimum yield of biodiesel. The result clearly shows that the optimal yield was obtained at 15 mg of catalyst concentration (**Figure 4**).

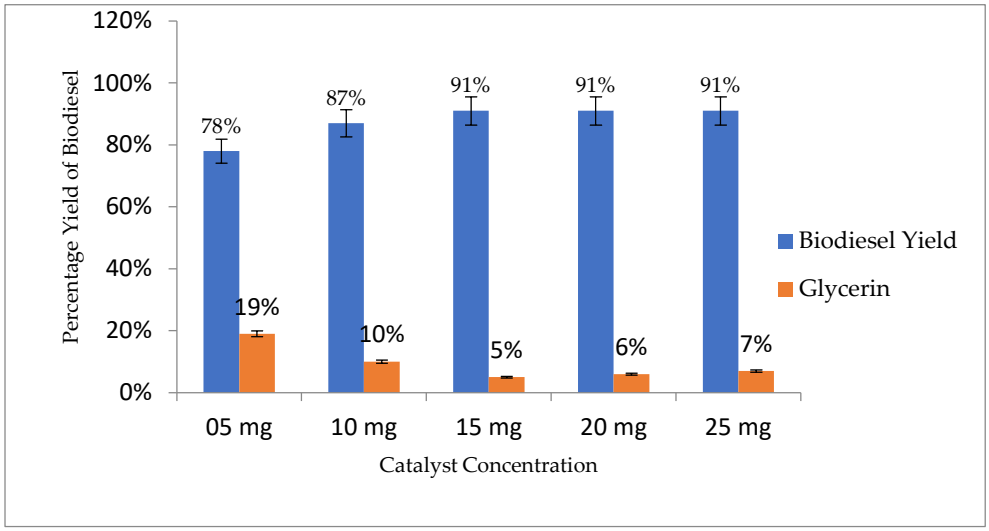

Figure 4. Catalyst concentration effect on biodiesel yield.

Preprints (www.preprints.org) | NOT PEER-REVIEWED | Posted: 19 July 2022 doi:10.20944/preprints202207.0278.v1

According to Bojan and Durairaj [31] and Leung and Guo [32], a high concentration of catalyst causes soap formation due to emulsification. Furthermore, the large amount of catalyst increases the viscosity of the reactants, which results in a reduction in the biodiesel yield [15].

3.4.3. Reaction Temperature

To synthesize biodiesel on a large scale in industries, low temperature is needed for transesterification because a high temperature leads to an increase in energy cost. Therefore, the reaction temperature requirement should be reduced; therefore, during the transesterification reaction, we have kept the reaction temperature at 45, 50, 55, 60, and 65 ^{0}C, respectively. The investigation findings evidently express the influence of temperature on biodiesel yield (**Figure 5**).. It was observed that when the temperature was increased from 55 ^{0}C to 60 ^{0}C the biodiesel yield rose to 91%.

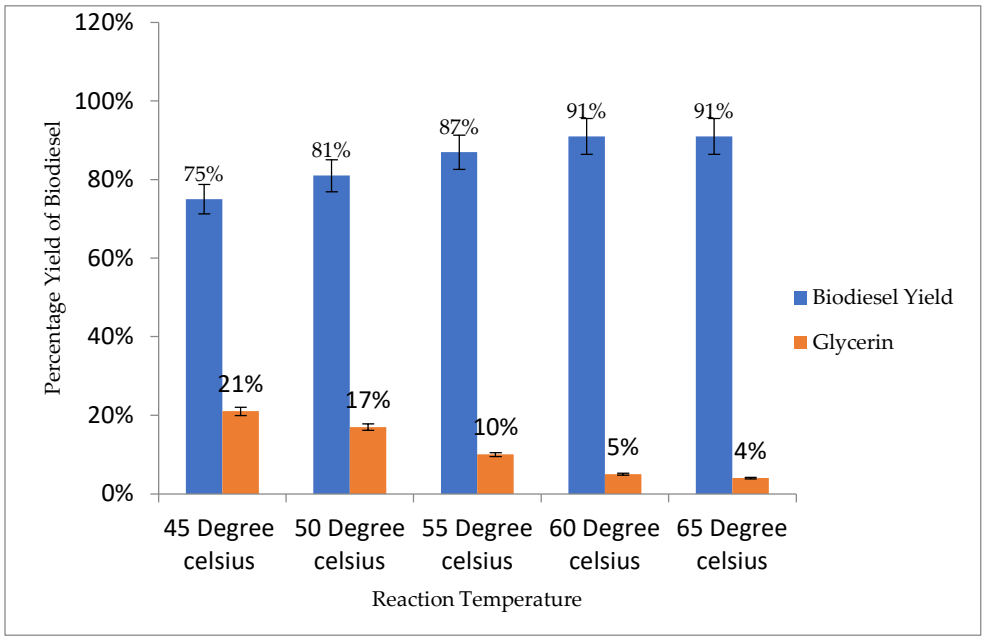

Figure 5. Influence of reaction temperature on the biodiesel yield and on the glycerin formation.

The reaction temperature markedly influenced the biodiesel yield, as a high reaction temperature increases the reaction speed and minimizes the duration of the reaction because it lowers the viscosity of the reaction medium, increases the solubility of alcohol and accelerates the transfer rates of the reagent [15,33,34]. Furthermore, other researchers have also reported almost similar results [15,34-36]. The decrease in biodiesel amount at high temperatures (more than 65 ^{0}C) may be due to the high miscibility that results in the reduction of phase separation as well as yield [15].

3.4.4. Reaction Time

To produce biodiesel on a large scale in industries, time is a primary parameter and should be minimized because extended reaction time increases energy expenditure and thus the cost of the product [34,37,38,39]. Therefore, we have also varied the duration of reaction in 20, 40, 60, 80 and 100 minutes, to determine the ideal time for optimum biodiesel yield by keeping other conditions constant. The result of this study clearly shows that an optimal yield (91%) of biodiesel was obtained at 45 minutes and no change in yield was observed at the reaction time of 60 and 75 minutes (**Figure 6**).

Preprints (www.preprints.org) | NOT PEER-REVIEWED | Posted: 19 July 2022 doi:10.20944/preprints202207.0278.v1

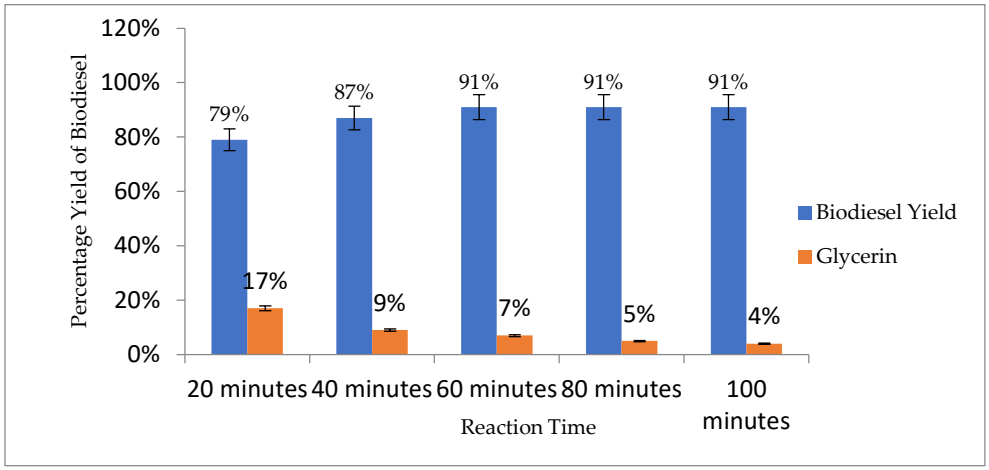

Figure 6. Influence of the reaction time on the biodiesel yield and on the glycerin formation reduction.

Similar results were stated by Ullah et al. [15], Barros et al. [34] Gebremariam and Marchetti, [38].

3.5. Physical and Fuel Properties of Biodiesel

SMB biodiesel prepared in this study, had a 0.74 mg KOH/g acid value that was below the standard range defined by ASTM D-644 (0.80 mg KOH/g). The acid value of SMB was more or less similar to the values reported by Vila Vázquez et al. [40]. The acid value of biodiesel is also influenced by its purity quality. Furthermore, the kinematic viscosity of SMB was calculated as 4.69 mm^2/s at 40 ^0C and is within the limit of the ASTM D-6751 standard. The kinematic viscosity of SMB was also found to be close to that of fossil diesel [15]. Moreover, the density of obtained SMB was 0.857 kg/l, which is within the ASTM D-6751 standards range [15,41]. According to Kaisan et al. [42] and Ullah et al. [15], due to high oxygen contents, SMB biodiesel has a lower calorific value than fossil diesel. The calorific value of SMB is also in the limit of ASTM D-6751 (**Table 1**).

The EN 14214 standard identified that biodiesel must have a flash point of more than 120 ^0C, while the ASTM D-6751 allows the range to be below 130 ^0C. The methanol content of any biodiesel has a pronounced effect on the flash point of biodiesel [15]. According to Ullah et al. [15], when the methanol content of biodiesel increases by 0.5%, its flash point decreases by 50 ^0C. The SMB flash point of in this study was calculated 87 ^0C (**Table 1**). This is within the EN 14214 and ASTM D 6751-02 standards range. According to previous studies, the range of flashpoints for biodiesel is 160-202 ^0C [43,44].

Cetane number of SMB was in this study determined as 49 (**Table 1**), which is just above the ASTM D-6751 standards. If the cetane number is above the limit, it is possible to adjust it by adding by a small amount of nitric acid iso-octyl, to achieve the conformation quality [11,45]. The statement indicates that there is an inverse proportionality between the degree of unsaturation of fatty acids and the number of cetane [15].

CP and PP of SMB were in this study, determined as -2 ^0C and -8 ^0C respectively. But there is no limit for CP and PP according to the ASTM D 6751 standard. However, Mofijur et al. [46] have specified a value for CP and PP. Sulfur content was in this study determined to be 0.00018 ppm, which is in the range limit of ASTM D 4294 (0.05 ppm). Therefore, SMB can be considered as an environmentally friendly fuel [15,28].

In the current study, we have also determined the oxidative stability of SMB and it was 2.8 minutes. This value was within the limit defined by ASTM D-6751 (3 minutes). Although, from an environmental perspective, the susceptibility to oxidation is desirable [47], but without a doubt oxidative stability is the main drawback and impeding its commercial use in vehicles. During storage or use, oxidation alters the tri-biological and physicochemical properties of biodiesel. The adverse effects of this phenomenon are incensement in insoluble deposits, acid number, density, iodine value, kinematic viscosity,

Preprints (www.preprints.org) | NOT PEER-REVIEWED | Posted: 19 July 2022 doi:10.20944/preprints202207.0278.v1

polymer content, and peroxide value. However, the oxidative instability of biodiesel can be minimized by adding various antioxidants [48,49]. Other researchers also reported almost same result in their study [17].

Another important aspect of fuel quality is its water content. As biodiesel is composed of fatty acid methyl esters (FAMEs), which are more hygroscopic, thus making the biodiesel more hydrophilic than fossil diesel. Therefore, biodiesel absorbs more moisture than fossil fuel. Free water favors biological growth in fuel tanks, which may result in fuel tank corrosion (made up of iron and steel), as well as slime and sludge formation, and consequently thus may lead to blockage of engine filters as well fuel pipes. This may damage the vehicle fuel injection system [50]. In this study, the water content for SMB was documented as 0.039, and it is below the limit specified by ASTM D-6751.

The degree of saturation and unsaturation and the oxidative stability of biodiesel are estimated from its iodine content value [51]. For the current biodiesel, the iodine content was observed 124, it is within the limit specified by ASTM D-6751. In this work, the refractive index was obtained as 1.437, which confirms the fact that crude oil is transformed into biodiesel during the transesterification reaction [52].

Another important fuel property of biodiesel is the higher heating value (HHV) that defines the fuel efficiency and energy content [53,54]. HHV can be estimated from the fatty acid composition, the iodine content, and the saponification value of biodiesel [54,55]. Biodiesel has HHV as have the fossil fuel. Biodiesel has HHV 39 to 43 MJ/kg, which is slightly lower than diesel (49.65 MJ/kg) [54,56]. The HHV of SMB was in the current study determined as 40.86 MJ/kg.

3.6. ^{1}H-NMR study of SMB

The characteristic singlet peak obtained at 3.667 ppm confirmed the presence of methoxy proton (-OCH_3). Furthermore, the alpha-methylene proton (α-CH_2) peaks were observed from 2.000 to 2.060 ppm. These two peaks confirmed the formation of FAMEs from triglycerides. The other important peaks observed were for terminal methyl protons (CH3) at 0.858-0.918 ppm. The next strong indication was the peak obtained from 1.254 to 1.682 ppm for beta-carbonyl methylene protons (**Figure 7**).

The presence of olefinic hydrogen [58], was confirmed by the multiple peaks obtained at 5.288-5.407 ppm. The obtained peaks confirm the successful transformation of triglycerides into FAMEs [15,57].

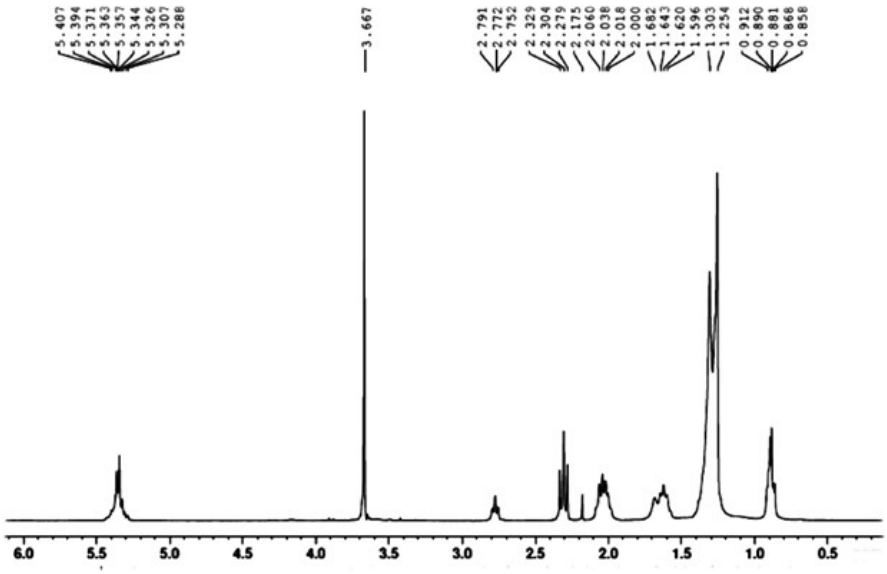

Figure 7. ^{1}H-NMR spectroscopy confirming the synthesis of biodiesel through various important peaks.

Preprints (www.preprints.org) | NOT PEER-REVIEWED | Posted: 19 July 2022 doi:10.20944/preprints202207.0278.v1

3.7. ^{13}C-NMR study of SMB

The presence of long-chain ethylene carbons (-CH_2-), was in this study confirmed by the occurrence of peaks at 24.93-34.22 ppm. Peaks at 172.71, 173.12 and 130.16 ppm confirmed carbonyl carbon (-CO) and unsaturation position in the SMB. Furthermore, the peak at 128.14 ppm is an indication of vinylic (C=H) substituent (**Figure 8**).

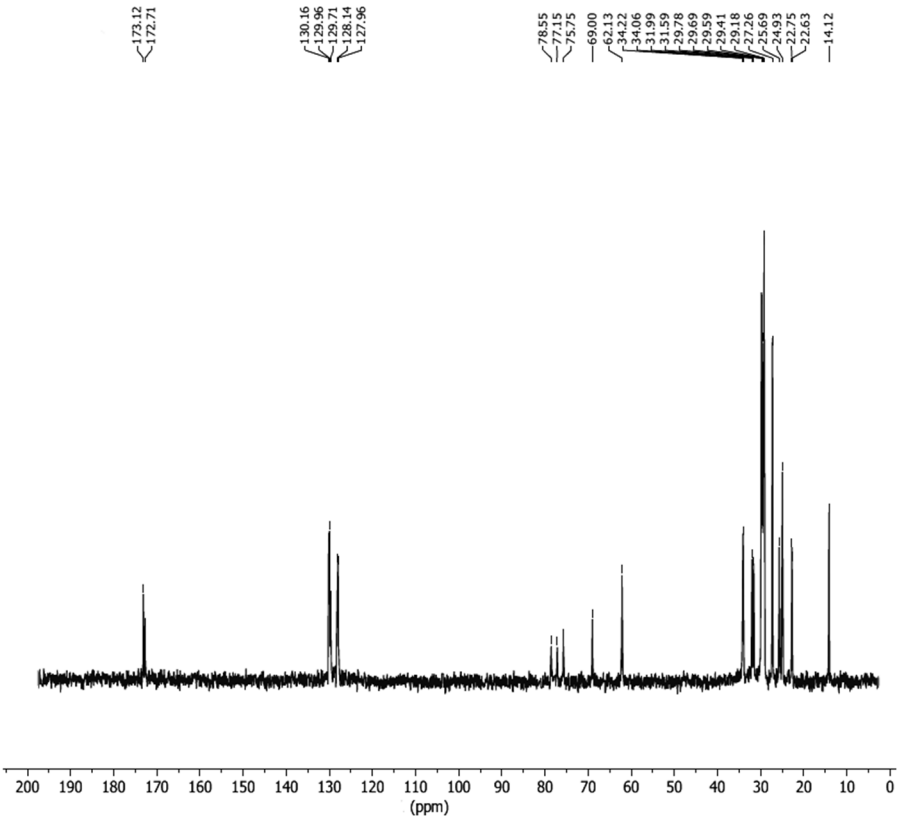

Figure 8. ^{13}C-NMR spectroscopy confirmation of transesterification process.

Peaks for these functional groups in the specified range were reported also in other studies [59].

3.8. Qualitative and Quantitative Analysis of SMB

Gas chromatography and mass spectroscopy were performed to study the composition of FAMEs produced during the transesterification process of biodiesel synthesis. The GC-MS results showed 19 peaks of different types of FAMEs. Every single peak represents a specific FAME and was confirmed through NIST 02 library match software. The retention time data identifies each FAME after mass spectrometric analysis (**Table 2**). The analysis showed that Linoleic acid methyl ester, Palmitic acid methyl ester, Oleic acid methyl ester, and Arachidic acid methyl ester are the major FAMEs identified in the SMB. The mass fragmentation patterns and retention time of the eluted components were used for the confirmation of various FAMEs. It is evident from the GC-MS data that the SMB is primarily composed of various FAMEs (**Figure 9)**.

Preprints (www.preprints.org) | NOT PEER-REVIEWED | Posted: 19 July 2022 doi:10.20944/preprints202207.0278.v1

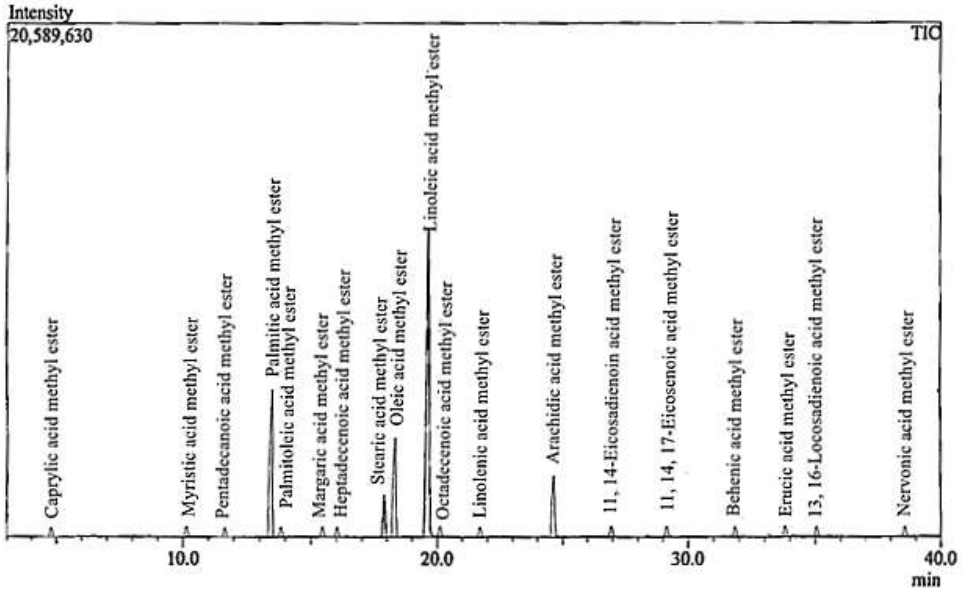

Figure 9. GC-MS analysis of SMB composition of different FAMEs formed in transesterification reaction.

In the present study, 19 different types of FAMEs in SMB were reported for the first time (**Table 2**). The presence of long-chain fatty acids of FAME profile are the indications of improved properties of biodiesel, and therefore, indorses high fuel efficiency [60]. While other researchers using the same feedstock reported less number of FAMEs such as Takase et al. [17] reported five FAMEs, Ullah et al., [59] reported seven FAMEs, and Fadhil et al. [18] reported six FAMEs.

Preprints (www.preprints.org) | NOT PEER-REVIEWED | Posted: 19 July 2022 doi:10.20944/preprints202207.0278.v1

Table 2. FAMEs composition of *Silybum marianum biodiesel* determined by GC-MS.

Identified FAMEs	Formula	CAS	RT	C
Caprylic acid methyl ester	$C_9H_{18}O_2$	111-11-5	4.739	0.16
Myristic acid methyl ester	$C_{15}H_{30}O_2$	124-10-7	10.168	0.34
Pentadecanoic acid methyl ester	$C_{16}H_{32}O_2$	7132-64-1	11.267	1.08
Palmitic acid methyl ester	$C_{17}H_{34}O_2$	112-39-0	13.424	16.11
Palmitoleic acid methyl ester	$C_{17}H_{32}O_2$	1120-25-8	13.878	0.12
Margaric acid methyl ester	$C_{18}H_{36}O_2$	1731-92-6	15.500	0.21
Heptadecenoic acid methyl ester	$C_{18}H_{36}O_2$	1731-92-6	15.943	0.27
Stearic acid methyl ester	$C_{19}H_{38}O_2$	112-61-8	17.897	2.33
Oleic acid methyl ester	$C_{19}H_{36}O_2$	112-62-9	18.375	8.52
Linoleic acid methyl ester	$C_{19}H_{34}O_2$	112-63-0	19.659	62.23
Octadecenoic acid methyl ester	$C_{19}H_{36}O_2$	1937-62-8	20.817	0.25
Linolenic acid methyl ester	$C_{19}H_{34}O_2$	112-63-0	21.743	0.31
Arachidic acid methyl ester	$C_{21}H_{42}O_2$	1120-28-1	24.661	4.47
11, 14-Eicosadienoic acid methyl ester	$C_{21}H_{38}O_2$	61012-46-2	26.948	0.39
11, 14, 17-Eicosenoic acid methyl ester	$C_{21}H_{40}O_2$	1120-28-1	29.259	0.81
Behenic acid methyl ester	$C_{23}H_{46}O_2$	929-77-1	31.994	0.83
Erucic acid methyl ester	$C_{23}H_{44}O_2$	1120-34-9	33.910	0.41
13, 16-Docosadienoic acid methyl ester	$C_{23}H_{42}O_2$	61012-47-3	35.030	0.19
Nervonic acid methyl ester	$C_{25}H_{48}O_2$	2733-88-2	38.611	0.97

CAS - Chemical Abstracts Service, RT - Retention Time (min), C - Concentration (%),

3.9. FT-IR Analysis of SMB

In the biodiesel samples for the identification of the various functional groups and types of binding linkages, corresponding to various vibrations of stretching and bending, FT-IR spectroscopy was used. Oils and esters are noted to be fairly strong absorbers in the infrared region of the electromagnetic spectrum [61,62]. Fourier transform infrared (FT-IR) spectroscopy has proven to be a powerful analytical tool for the identification of macromolecular pools (e.g., proteins, lipids, and carbohydrates) and in the monitoring of biochemical changes [63]. According to Soon et al. [64], the position of the carbonyl group is sensitive to the molecular structure as well as substituent effects. In the FT-IR spectroscopy of the SMB, the stretch for terminal (vinyl) C-H was observed at 3011cm^{-1}. Stretching bands for methyl and methylene were attained at 2856 cm^{-1} and 2926 cm^{-1}, respectively. The methoxycarbonyl (methyl ester) group was observed at 1742 cm^{-1}. The stretching for alkenyl was obtained at 1648 cm^{-1}. The peaks for Methyl C-H bend were obtained at 1436 cm^{-1} and 1463 cm^{-1}. The peak of the aromatic tertiary amine C-H stretch was obtained at 1360 cm^{-1}. The peak for aromatic ether (aryl–O stretching) was obtained at 1245 cm^{-1}. Stretching for organic sulfates was obtained at 1198 cm^{-1}. The stretching peak obtained at 1172 cm^{-1} is for the secondary amine (C-N). The peak of the cyclohexane ring C-O was obtained at 1018 cm^{-1}. The peak methine of skeletal C-C vibration was obtained at 913 cm^{-1}. The peak for vinylidene C-H in the plan was obtained at 883 cm^{-1}. The peak of peroxide C-O-O stretch was observed at 843 cm^{-1}. The peak of methylene –$(CH_2)_n$– rocking was

Preprints (www.preprints.org) | NOT PEER-REVIEWED | Posted: 19 July 2022 doi:10.20944/preprints202207.0278.v1

obtained at 722 cm^{-1}. The peak obtained at 831.51 cm^{-1} confirmed the presence of the C-O-O stretch and the last peak obtained at 603 cm^{-1} is for disulfide stretch (S-S) (**Figure 10**) [65].

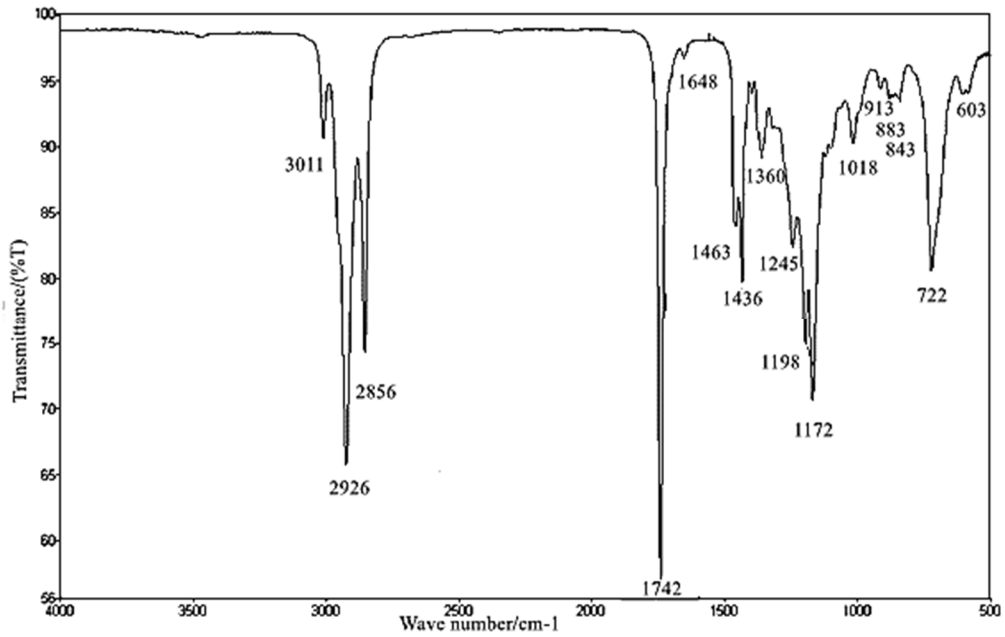

Figure 10. FT-IR spectroscopy result confirming SMB formation by peaks for important functional groups.

FTIR spectroscopic study was performed to confirm the biodiesel synthesis and to confirm various functional groups formed during the transesterification process. There are two main peaks for ester formation; one is carbonyl, for which the peak range is 1725-1750 cm^{-1}, and the other is C-O, for which the peak range is 1000-1300 cm^{-1} [15]. Another strong characteristic peak obtained at 1245 cm^{-1} also confirms the formation of methyl esters [66,67]. The peaks obtained in FT-IR spectroscopy confirm that the transesterification process occurred successfully, and it is also a suitable method for the conversion of triglyceride to fatty acid methyl esters [68,69].

4. Conclusions

In the near future, due to the increase in demand for the energy and depletion of fossil fuels reservoirs the demand for biodiesel is expected to increase rapidly. *Silybum marianum* (L.) Gaertn., commonly known as milk thistle, is an annual herb of the family Asteraceae. In this study, the transesterification technique was used to synthesize biodiesel using *Silybum marianum* as feedstock and ZnO as catalyst. The oil content of the feedstock was 45.2% with acid value of 0.74 mg KOH/g. To get optimum yield of biodiesel five-five variables were taken of the parameters oil to methanol molar ratio, catalyst concentration, reaction temperature and reaction time. The optimum yield of 91% was obtained at 1:24 of oil to methanol ratio, 15 mg of catalyst concentration, 60 ^{0}C temperature and 45 minutes of reaction time. The fuel properties were tested through standard methods of ASTM and were found within the limits specified by ASTM D-6751. ^{1}*H-NMR* and ^{13}*C-NMR*, GC-MS and FT-IR spectroscopies were performed to confirm the successful occurrence of transesterification process. All physicochemical characteristics clearly showed that the *Silybum marianum* could be a potential non-edible feedstock for the biodiesel industry because it is economical, indigenously available, and environmentally friendly and can be easily grown in various environmental conditions.

Author Contributions: All authors declare to have equal, direct, and intellectual contributions and have approved the current work for publication in this journal.

Conflicts of Interest: The authors declare no conflict of interest. The funders had no role in the design of the study; in the collection, analyses, or interpretation of data; in the writing of the manuscript; or in the decision to publish the results.

Acknowledgment: This study was partially supported by the Slovak Research and Development Agency under the contracts APVV-14-0393 and APVV-16-0088.

Funding: This research received no external funding.

Data Availability Statement: Not applicable.

Abbreviations

ASTM - American Society for Testing and Materials
CP - Cloud Point
FAME - Fatty Acid Methyl Esters
FFA - Free Fatty Acid
GC-MS – Gas Chromatography-Mass Spectrometry
FT-IR spectroscopy – Fourier Transform Infrared Spectroscopy
H and C-NMR - *Nuclear Magnetic Resonance*
HHV - Higher Heating Value
PMCC - Flash Point (Pensky-Martens Closed Cup)
PP - Pour Point
SEM - Scanning Electron Microscopy
SMB - Silybum Marianum Biodiesel
XRD - X-Rays Diffraction
ZnO - Zinc Oxide

References

1. Zahed, M.A., Revayati, M., Shahcheraghi, N., Maghsoudi, F., Tabari, Y., 2021. Modeling and optimization of biodiesel synthesis using TiO_2–ZnO nanocatalyst and characteristics of biodiesel made from waste sunflower oil. *Curr. Res. Green and Sust. Chem.* 4, 100223. https://doi.org/10.1016/j.crgsc.2021.100223
2. Balat, M., Balat, H., 2010. Progress in biodiesel processing. *App. Ener.* 87, 1815-1835.
3. El-Mashad, H.M., Zhang, R., Avena-Bustillos, R.J. 2008. A two-step process for biodiesel production from salmon oil. *Biosys. Engin.* 99, 220-227.
4. Alptekin, E., Canakci, M., 2010. Optimization of pretreatment reaction for methyl ester production from chicken fat. *Fuel.* 89, 4035-4039.
5. Ramirez-Ortiz, J., Martinez, M., Flores, H., 2012. Metakaolinite as a catalyst for biodiesel production from waste cooking oil. *Front. Chem. Sci. & Eng. 6*(4), 403-409.
6. Narasimhan, M., Chandrasekaran, M., Govindasamy, S., Aravamudhan, A., 2021. Heterogeneous nanocatalysts for sustainable biodiesel production: A review. *J. Environ. Chem. Eng. 9*(1), 104876.
7. Toledo Arana, J., Torres, J.J., Acevedo, D.F., Illanes, C.O., Ochoa, N.A., Pagliero, C.L., 2019. One-step synthesis of CaO-ZnO efficient catalyst for biodiesel production. *Inter. J. Chem. Eng.* https://doi.org/10.1155/2019/1806017
8. Deshmane, V.G., Gogate, P.R., Pandit, A.B., 2009. Ultrasound-assisted synthesis of biodiesel from palm fatty acid distillate. *Ind. & Eng. Chem. Res.* 48(17), 7923-7927.
9. Gole, V.L., Gogate, P.R., 2012. Intensification of synthesis of biodiesel from nonedible oils using sonochemical reactors. *Ind. & Eng. Chem. Res.* 51(37), 11866-11874.
10. Bohlouli, A., Mahdavian, L., 2021. Catalysts used in biodiesel production: a review. *Biofuels.* 12(8), 885-898.
11. Khan, M.A., Blackshaw, R.E., Marwat, K.B., 2009. Biology of milk thistle (Silybum marianum) and the management options for growers in north-western Pakistan. *Weed Bio. & Manag.* 9(2), 99-105.
12. Thema, F.T., Manikandan, E., Dhlamini, M.S., Maaza, M.J.M.L., 2015. Green synthesis of ZnO nanoparticles via Agathosma betulina natural extract. *Mater. Lett*. 161, 124-127.
13. Sadiq, H., Sher, F., Sehar, S., Lima, E.C., Zhang, S., Iqbal, H.M., Nuhanović, M. 2021. Green synthesis of ZnO nanoparticles from Syzygium Cumini leaves extract with robust photocatalysis applications. *J. Molec. Liq.* 335, 116567.
14. Joshi, A., Singhal, P., Bachheti, R.K., 2011. Physicochemical characterization of seed oil of Jatropha curcus L. from Dehradun (Uttarakhand) Indian. *J. Appl. Biol. Pharm. Technol.* 2:123e7.
15. Ullah, K., Jan, H.A., Ahmad, M., Ullah, A., 2020. Synthesis and structural characterization of biofuel from Cocklebur sp., using zinc oxide nano-particle: A novel energy crop for bioenergy industry. *Front. Bioengin. Biotech.* 8, 756, https://doi.org/10.3389/fbioe.2020.00756
16. Birla, A., Singh, B., Upadhyay, S., Sharma, Y., 2012. Kinetics studies of synthesis of biodiesel from waste frying oil using a heterogeneous catalyst derived from snail shell. *Bioresource Technol*. 106, 95–100.

17. Takase, M., Feng, W., Wang, W., Gu, X., Zhu, Y., Li, T., Wu, X., 2014. Silybum marianum oil as a new potential non-edible feedstock for biodiesel: A comparison of its production using conventional and ultrasonic assisted method. *Fuel Process. Tech.* 123, 19-26.
18. Fadhil, A.B., Ahmed, K.M., Dheyab, M.M., 2017. Silybum marianum L. seed oil: A novel feedstock for biodiesel production. *Arab. J. Chem.* 10, 683-690.
19. Samanta, S., Sahoo, R.R., 2021. Waste cooking (palm) oil as an economical source of biodiesel production for alternative green fuel and efficient lubricant. *BioEner. Res.* 14(1), 163-174.
20. Gowthambabu, V., Balamurugan, A., Satheeshkumar, S., Kanmani, S.S., 2021. ZnO nanoparticles as efficient sunlight driven photocatalyst prepared by solution combustion method involved lime juice as biofuel. *Spectrochim. Acta Part A: Molec. & Biomolec. Spect. 258*, 119857.
21. Theivasanthi, T., Alagar, M., 2011. Nano sized copper particles by electrolytic synthesis and characterizations. *Inter. J. Phy. Sci.* 6(15), 3662-3671. https://doi.org/10.5897/IJPS10.116
22. Palanisamy, V.K., Manoharan, K., Raman, K., Sundaram, R., 2020. Efficient sunlight-driven photocatalytic behavior of zinc sulfide nanorods towards Rose Bengal degradation. *J. Mater. Sci. Mater. in Elect.* 31(17), 14795-14809.
23. Fan, M., Liu, Y., Zhang, P., Jiang, P., 2016. Blocky shapes Ca-Mg mixed oxides as a water-resistant catalyst for effective synthesis of biodiesel by transesterification. *Fuel Pro. Tech.* 149, 163-168.
24. Awual, M.R., Yaita, T., Shiwaku, H., 2013. Design a novel optical adsorbent for simultaneous ultra-trace cerium (III) detection, sorption and recovery. *Chem. Eng. J.* 228, 327-335.
25. Takase, M., Zhang, M., Feng, W., Chen, Y., Zhao, T., Cobbina, S.J., Wu, X., 2014. Application of zirconia modified with KOH as heterogeneous solid base catalyst to new non-edible oil for biodiesel. *Ener. Conv. & Manag.* 80, 117-125.
26. Worapun, I., Pianthong, K., Thaiyasuit, P., 2012. Two-step biodiesel production from crude Jatropha curcas L. oil using ultrasonic irradiation assisted. *J. Oleo. Sci.* 61, 165-172. https://doi.org/10.5650/jos.61.165
27. Meher, L., Vidya Sagar, D., Naik, S., 2006. Technical aspects of biodiesel production by transesterification-a review. *Renew. Sustain. Ener. Rev.* 10, 248–68.
28. Kumar, K., 2013. Standardization of non-edible Pongamia pinnata oil methyl ester conversion using hydroxyl content and GC–MS analysis. *J. Taiw. Ins. Chem. Eng.* 45(4), 1485-1489. https://doi.org/10.1016/j.jtice.2013.11.002
29. Miao, X., Wu, Q., 2006. Biodiesel production from heterotrophic microalgal oil. *Biores. Tech.* 97, 841–846. https://doi.org/10.1016/j.biortech.2005.04.008
30. Encinar, J.M., González, J.F., Sabio, E., Ramiro, M.J., 1999. Preparation and properties of biodiesel from Cynara C arduncu-lus L. oil. *Ind. Eng. Chem. Res.* 38, 2927–31.
31. Bojan, S.G., Durairaj, S.K., 2012. Producing Biodiesel from High Free Fatty Acid Jatropha Curcas Oil by A Two Step Method-An Indian Case Study. *J. Sust. Ener. Environ.* 3, 63-66.
32. Leung, D.Y.C., Guo, Y., 2006. Transesterification of neat and used frying oil: optimization for biodiesel production. *Fuel Process. Tech.* 87(10), 883-890.
33. Silva, C.D., Oliveira, J.V., 2014. Biodiesel production through non-catalytic supercritical transesterification: current state and perspectives. *Braz. J. Chem. Eng.* 31, 271-285.
34. Barros, S.D.S., Junior, W.A.P., Sá, I.S., Takeno, M.L., Nobre, F.X., Pinheiro, W., de Freitas, F.A., 2020. Pineapple (Ananás comosus) leaves ash as a solid base catalyst for biodiesel synthesis. *Biores. Tech.* 312, 123569.
35. Phan, A.N., Phan, T.M., 2008. Biodiesel production from waste cooking oils. *Fuel.* 87(17-18), 3490-3496.
36. Zhang, Y., Dubé, M.A., McLean, D.D., Kates, M., 2003. Biodiesel production from waste cooking oil: 2. Economic assess-ment and sensitivity analysis. *Biores. Tech.* 90(3), 229-240.
37. Mathiyazhagan, M., Ganapathi, A., 2011. Factors affecting biodiesel production. *Res. Plant Bio.* 1(2), 1-5. https://doi.org/10.1016/S0960-8524(03)00150-0
38. Gebremariam, S.N., Marchetti, J.M., 2018. Economics of biodiesel production. *Ener. Conver. & Manag.* 168, 74-84.
39. Dhawane, S.H., Karmakar, B., Ghosh, S., Halder, G., 2018. Parametric optimisation of biodiesel synthesis from waste cook-ing oil via Taguchi approach. *J. Environ. Chem. Engin.* 6(4), 3971-3980.
40. Ávila Vázquez, V., Díaz Estrada, R.A., Aguilera Flores, M.M., Escamilla Alvarado, C., Correa Aguado, H.C., 2020. Trans-esterification of non-edible castor oil (Ricinus communis L.) from Mexico for biodiesel production: a physicochemical characterization. *Biofuels* 11(7), 753-762.
41. Wang, R., Hanna, M.A., Zhou, W.W., Bhadury, P.S., Chen, Q., Song, B.A., Yang, S., 2011. Production and selected fuel properties of biodiesel from promising non-edible oils: Euphorbia lathyris L., Sapium sebiferum L. and Jatropha curcas L. *Biores. Tech.* 102, 1194-1199. https://doi.org/10.1016/j.biortech.2010.09.066
42. Kaisan, M.U., Anafi, F.O., Nuszkowski, J., Kulla, D.M., Umaru, S., 2017. Calorific value, flash point and cetane number of biodiesel from cotton, jatropha and neem binary and multi-blends with diesel. Biofuels. https://doi.org/10.1080/17597269.2017.1358944
43. Refaat, A.A., Attia, N.K., Sibak, H.A., El Sheltawy, S.T., El Diwani, G.I., 2008. Production optimization and quality assess-ment of biodiesel from waste vegetable oil. *Int. J. Environ. Sci. Tech.* 5, 75-82. https://doi.org/10.1007/BF03325999
44. Dias, J.M., Alvim-Ferraz, M., Almeida, M.F., 2008. Comparison of the performance of different homogeneous alkali cata-lysts during transesterification of waste and virgin oils and evaluation of biodiesel quality. *Fuel*. 87, 3572-3578. https://doi.org/10.1016/j.fuel.2008.06.014

45. Knothe, G., 2009. Improving biodiesel fuel properties by modifying fatty ester composition. *En. Environ. Sci.* 2, 759–766. https://doi.org/10.1039/B903941D
46. Mofijur, M., Masjuki, H.H., Kalam, M.A., Rasul, M.G., Atabani, A.E., Hazrat, M.A., Mahmudul, H.M., 2015. Effect of biodiesel-diesel blending on physico-chemical properties of biodiesel produced from Moringa oleifera. *Procedia. Eng.* 105, 665-669. https://doi.org/10.1016/j.proeng.2015.05.046
47. Bagher, A.M., Vahid, A., Mohsen, M., Reza, B.M., 2016. Effect of Using Renewable Energy in Public Health. *Amer. J. En. Sci.* 3(1), 1-9.
48. Kumar, N., 2017. Oxidative stability of biodiesel: Causes, effects and prevention. *Fuel*. 190, 328-350.
49. Bannister, C.D., Chuck, C.J., Bounds, M., Hawley, J.G., 2011. Oxidative stability of biodiesel fuel. *P I MECH ENG D-J AUT.* 225(1), 99-114.
50. Fregolente, P.B.L., Fregolente, L.V., Wolf Maciel, M.R., 2012. Water content in biodiesel, diesel, and biodiesel–diesel blends. *J. Chem. & Engin. Dat*. 57(6), 1817-1821.
51. da Costa Cardoso, L., de Almeida, F.N.C., Souza, G.K., Asanome, I.Y., Pereira, N.C., 2019. Synthesis and optimization of ethyl esters from fish oil waste for biodiesel production. *Renew. Ener. 133*, 743-748.
52. Lugo-Méndez, H., Sánchez-Domínguez, M., Sales-Cruz, M., Olivares-Hernández, R., Lugo-Leyte, R., Torres-Aldaco, A., 2021. Synthesis of biodiesel from coconut oil and characterization of its blends. *Fuel*. 295, 120595.
53. Demirbaş, A., 2003. Biodiesel fuels from vegetable oils via catalytic and non-catalytic supercritical alcohol transesterifications and other methods: a survey. *Ener. Conver. & Manag.* 44(13), 2093-2109.
54. Sivaramakrishnan, K., Ravikumar, P., 2011. Determination of higher heating value of biodiesels. *Inter. J. Engin. Sci. & Tech.* 3(11), 7981-7987.
55. Anand, K., Ranjan, A., Mehta, P.S., 2010. Estimating the viscosity of vegetable oil and biodiesel fuels. *Ener. & fuels*. 24(1), 664-672.
56. Demirbaş, A., 2008. Production of biodiesel from algae oils. *Ener. Sour. Part A: Rec. Utili. & Environ. Eff.* 31(2), 163-168.
57. Portela, N.A., Oliveira, E.C., Neto, A.C., Rodrigues, R.R., Silva, S.R., Castro, E.V., Filgueiras, P.R., 2016. Quantification of biodiesel in petroleum diesel by 1H NMR: evaluation of univariate and multivariate approaches. *Fuel*. 166, 12-18.
58. Knothe, G., 2000. Monitoring a progressing transesterification reaction by fiber optic NIR spectroscopy with correlation to 1H NMR spectroscopy. *J. Am. Oil. Chem. Soc.* 77, 489e93.
59. Ullah, K., Ahmad, M., Qiu, F., 2015. Assessing the experimental investigation of milk thistle oil for biodiesel production using base catalyzed transesterification. *Ener.* 89, 887-895.
60. Asci, F., Aydin, B., Akkus, G.U., Unal, A., Erdogmus, S.F., Korcan, S.E., Jahan, I., 2020. Fatty acid methyl ester analysis of Aspergillus fumigatus isolated from fruit pulps for biodiesel production using GC-MS spectrometry. *Bioengin.* 11(1), 408-415.
61. O'Donnell, S., Demshemino, I., Yahaya, M., Nwadike, I., Okoro, L., 2013. A review on the spectroscopic analyses of biodiesel. *European Inter. J. Sci. & Tech. 2*(7), 137-146.
62. Atabani, A.E., Shobana, S., Mohammed, M.N., Uğuz, G., Kumar, G., Arvindnarayan, S., Ala'a, H., 2019. Integrated valorization of waste cooking oil and spent coffee grounds for biodiesel production: Blending with higher alcohols, FT–IR, TGA, DSC and NMR characterizations. *Fuel*. 244, 419-430.
63. Miglio, R., Palmery, S., Salvalaggio, M., Carnelli, L., Capuano, F., Borrelli, R., 2013. Microalgae triacylglycerols content by FT-IR spectroscopy. *J. App. Phycol.* 25(6), 1621-1631.
64. Soon, L.B., Rus, A.Z.M., Hasan, S., 2013. Continuous biodiesel production using ultrasound clamp on tubular reactor. *Inter. J. Auto. Mech. Eng.* 8(1), 1396-1405.
65. Nandiyanto, A.B.D., Oktiani, R., Ragadhita, R., 2019. How to read and interpret FTIR spectroscope of organic material. *Indon. J. Sci. & Tech.* 4(1), 97-118.
66. Siatis, N.G., Kimbaris, A.C., Pappas, C.S., Tarantilis, P.A., Polissiou, M.G. 2006. Improvement of biodiesel production based on the application of ultrasound: monitoring of the procedure by FTIR spectroscopy. *J. Amer. Oil Chem. Soci.* 83(1), 53-57.
67. Taufiq-Yap, Y.H., Abdullah, N.F., Basri, M., 2011. Biodiesel production via transesterification of palm oil using NaOH/Al2O3 catalysts. *Sains Malay.* 40(6), 587-594.
68. Andrade, T.A., Errico, M., Christensen, K.V. 2017. Transesterification of castor oil catalyzed by liquid enzymes: Optimization of reaction conditions. In *Computer Aided Chemical Engineering* (Vol. 40, pp. 2863-2868). Elsevier.
69. Elango, R.K., Sathiasivan, K., Muthukumaran, C., Thangavelu, V., Rajesh, M., Tamilarasan, K., 2019. Transesterification of castor oil for biodiesel production: Process optimization and characterization. *Microchem. J.* 145, 1162-1168.